Cancer Nanotechnology

DOI: 10.1002/anie.201402189

Conjugated-Polyelectrolyte-Based Polyprodrug: Targeted and Image-Guided Photodynamic and Chemotherapy with On-Demand Drug Release upon Irradiation with a Single Light Source**

*Youyong Yuan, Jie Liu, and Bin Liu**

Abstract: *Nanomaterials that combine diagnostic and therapeutic functions within a single nanoplatform are highly desirable for molecular medicine. Herein we report a novel theranostic platform based on a conjugated-polyelectrolyte (CPE) polyprodrug that contains functionality for image, chemo- and photodynamic therapy (PDT), and on-demand drug release upon irradiation with a single light source. Specifically, the PEGylated CPE serves as a photosensitizer and a carrier, and is covalently conjugated to doxorubicin through a linker that can be cleaved by reactive oxygen species (ROS). Under appropriate light irradiation, the CPE can generate ROS, not only for PDT, but also for on-demand drug release and chemotherapy. This nanoplatform will offer on-demand PDT and chemotherapy with drug release triggered by one light switch, which has great potential in cancer treatment.*

Multifunctional nanomaterials in which medical diagnostics, drug delivery, and efficient therapy (theranostics) are integrated into a single nanodelivery system have emerged as promising tools in personalized medicine.[1] These so-called image-guided systems are particularly useful for photoregulated cancer therapy, as the tumor can be monitored, and then light can be precisely applied to the detected region while leaving normal tissues untouched.[2] Tumor-targeting strategies have also been widely used to enhance the accumulation of nanocarriers at tumor sites through conjugating appropriate targeting moieties to the delivery systems.[3]

Photodynamic therapy (PDT), a photoregulated noninvasive medical technology, has been widely utilized for cancer therapy through the generation of reactive oxygen species (ROS) to destroy cancer cells upon the illumination of photosensitizers (PSs).[4] To enable a better therapeutic outcome, novel concepts of combining PDT and chemotherapy have been developed.[5] The combination of two therapeutic modalities is helpful in overcoming limitations encountered by each therapy when used alone. For example, the combination of PDT with chemotherapy has the potential to induce antitumor immunity[6] or revert multidrug resistance.[5c] Current delivery systems are largely based on the coloading of both PSs and chemotherapeutic drugs into the same carrier. The drugs in these systems are uncontrollable, which could readily lead to side effects with limited therapeutic efficiency owing to premature burst drug release in the blood circulation as well as slow diffusional release after their accumulation at the tumor site. As a consequence, the development of drug-delivery systems that show "on-demand" drug release only at the targeted site is much preferred. Stimuli-responsive nanocarriers have been developed for "triggered" drug release through activation by environmental stimuli.[7] Among these stimuli, light has attracted much attention because it is an orthogonal external stimulus that provides the advantages of a noncontact mode and precise controllability, as well as the controlled release of encapsulated substances both spatially and temporally.[8] However, as most light-responsive systems are activated by UV light, whereas the majority of PSs respond to visible light, two light sources are often needed to activate each for combined chemotherapy and PDT. Sequential irradiation makes it difficult to focus the two light beams on the same position. It remains challenging to develop a platform for combined chemotherapy and PDT with on-demand drug release upon irradiation with a single light source.

Conjugated polyelectrolytes (CPEs) have attracted great attention for sensing and image applications.[9] In comparison with small-organic-molecule dyes, the backbone of CPEs has a great number of light-absorbing units, which result in high absorption coefficients and bright fluorescence under irradiation with light. This feature, together with their great biocompatibility and good photostability, make them a new generation of bioimage agents.[9] Furthermore, some CPEs were also found to be able to generate ROS under appropriate irradiation with light, and were successfully used for PDT and antimicrobial study.[10] Recent reports that thioketal groups can be readily cleaved by ROS[11] inspired us to develop a nanoplatform that combines PDT and chemotherapy with on-demand drug release regulated by one light source. Such a system can be constructed by introducing a ROS-cleavable linker between the PS and the drug; upon illumination, the generated ROS causes drug release through the cleavage of the linker. Although intracellular ROS are an indicator of cancer, in view of their low concentration in cells as well as their short lifetime (< 0.1 ms) and limited range of action (10–20 nm), it should be more effective to generate ROS in situ by the use of a ROS-sensitive drug-delivery system.

[*] Dr. Y. Yuan, Dr. J. Liu, Prof. Dr. B. Liu
Department of Chemical and Biomolecular Engineering
National University of Singapore
4 Engineering Drive 4, Singapore, 117576 (Singapore)
E-mail: cheliub@nus.edu.sg
Prof. Dr. B. Liu
Institute of Materials Research and Engineering
3 Research Link, Singapore 117602 (Singapore)

[**] We thank the Singapore National Research Foundation (R-279-000-390-281), the Ministry of Defense (R279-000-340-232), and the JCO (IMRE12-8P1103).

Supporting information for this article is available on the WWW under http://dx.doi.org/10.1002/anie.201402189.

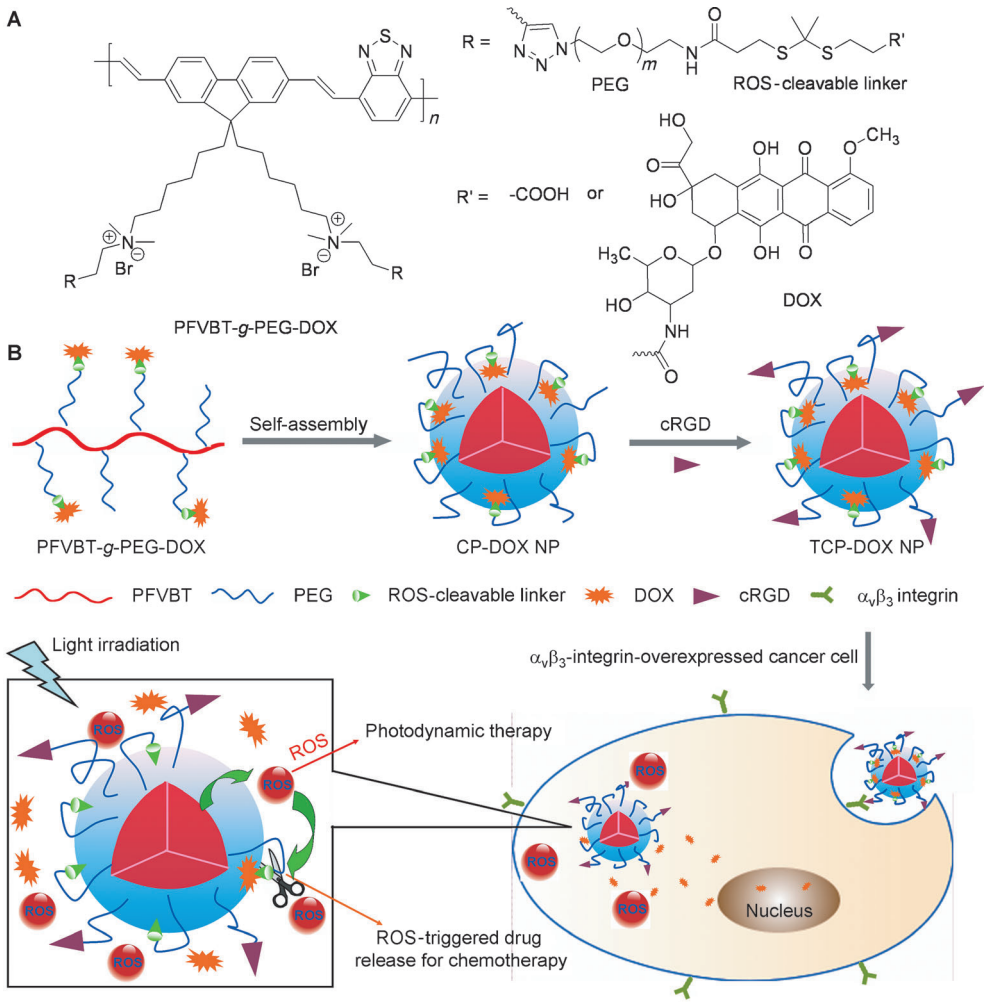

Scheme 1. A) Chemical structure of the PEGylated polyprodrug PFVBT-*g*-PEG-DOX and B) schematic illustration of the light-regulated ROS-activated on-demand drug release and the combined chemo–photodynamic therapy. PEG = poly(ethylene glycol).

Herein, we describe the development of a CPE–doxorubicin (DOX) polyprodrug for targeted and image-guided on-demand PDT and chemotherapy upon irradiation with one light. DOX was conjugated to a PEGylated polymeric PS through a ROS cleavable linker (Scheme 1). The obtained polyprodrug self-assembled into nanoparticles (NPs) in aqueous media, and the surface was further functionalized with a cyclic arginine–glycine–aspartic acid tripeptide (cRGD), which targets cancer cells in which $\alpha_v\beta_3$ integrin is overexpressed. Under irradiation with light, these NPs can generate ROS efficiently for PDT. Meanwhile, the generated ROS can quickly cleave the linker that covalently attaches DOX to the PS for specific on-demand drug release. As compared to existing systems, our "all-in-one" polyprodrug based on a single CPE contains all the functionalities required for image, therapy, and on-demand drug release.

For the synthesis of PFVBT-*g*-PEG-DOX (see Scheme S1 in the Supporting Information), the ROS-cleavable thioketal (TK) linker was first prepared, and one of its carboxy groups reacted with the amine group of a bifunctional poly(ethylene glycol) derivative (N_3-PEG-NH_2) to yield N_3-PEG-TK. N_3-PEG-TK was further treated with DOX to yield a mixture of N_3-PEG-TK-DOX and N_3-PEG-TK. An equimolar mixture of N_3-PEG-TK and DOX was used for conjugation, and about 70% of the carboxy groups reacted with DOX as based on NMR spectra. The unreacted carboxy groups enabled further attachment of the target moiety after self-assembly. Poly[9,9-bis(*N*-but-3′-ynyl-*N*,*N*-dimethylaminohexyl)-fluorenyldivinylene-*alt*-4,7-(2′,1′,3′,-benzothiadiazole) dibromide] (PFVBT) with alkyne side groups was synthesized according to our previously reported procedure.[12] This polymer underwent a subsequent click reaction with N_3-PEG-TK-DOX and a N_3-PEG-TK mixture to yield PFVBT-*g*-PEG-DOX. The DOX content in the conjugate was calculated to be 12.3 wt% as based on the integrated areas of the peak at 3.62 ppm (assigned to the methylene hydrogen atoms of PEG) and the peak at 0.56 ppm (assigned to the methylene hydrogen atoms nearest to the 9-position of fluorene) in the NMR spectrum. The brush polymer prepared by the click reaction between PFVBT and N_3-PEG-TK is denoted as PFVBT-*g*-PEG.

We used high-performance liquid chromatography (HPLC) to monitor drug release from N_3-PEG-TK-DOX in the presence of ROS produced by the reaction of H_2O_2 with Fe^{2+}. N_3-PEG-TK-DOX exhibited a monodispersed peak at an elution time of 3.5 min (Figure 1 A). Since the HPLC eluent contained 0.1% trifluoroacetic acid, we also incubated N_3-PEG-TK-DOX in water at pH 1.0 for 6 h. N_3-PEG-TK-DOX showed no degradation, thus demonstrating good stability of the thioketal linker under acidic conditions.[11a] The treatment of N_3-PEG-TK-DOX with ROS led to complete degradation of the thioketal linker and resulted in a single peak with an elution time of 4.9 min. This peak showed a mass-to-charge ratio (*m*/*z*) of 632.266, corresponding to sulfhydryl-modified doxorubicin (see Figure S1 in the Supporting Information). Although a short thiol ligand (3-mercaptopropanone) is attached to DOX after drug release, previous studies demonstrated that the DOX derivative is as potent as the parent drug.[13]

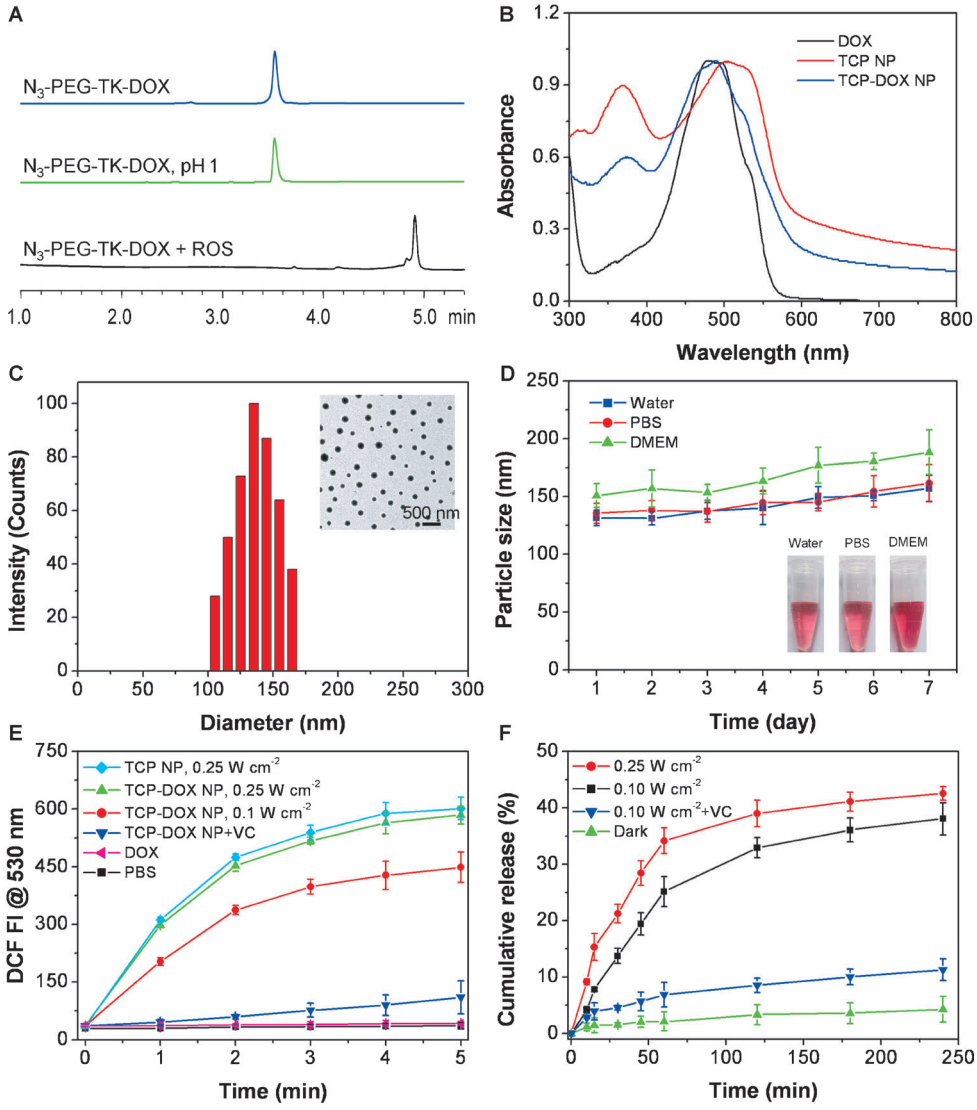

Figure 1. A) Analysis of the stability and degradation of N_3-PEG-TK-DOX in the presence of ROS, as detected by the absorbance at 254 nm by HPLC. B) Normalized UV/Vis absorption spectra of DOX, TCP NPs, and TCP-DOX NPs. C) Size distribution and TEM image (inset) of TCP-DOX NPs. D) Average size changes of TCP-DOX NPs when incubated in water, PBS buffer, or DMEM for 7 days. The inset shows photographs of TCP-DOX NPs dispersed in water, PBS buffer, or DMEM at day 7. E) Fluorescence intensity (FI) of DCF at 530 nm in PBS, with DOX in PBS, with TCP-DOX NPs in PBS, and with TCP NPs in PBS after irradiation with light for different amounts of time. VC stands for the ROS scavenger vitamin C. F) Cumulative release profiles of DOX from TCP-DOX NPs with and without irradiation with light. Standard deviations are shown as error bars for three parallel experiments.

PFVBT-*g*-PEG-DOX self-assembled into NPs (denoted as CP-DOX NPs) through a dialysis method. As carboxy groups are located at the terminus of the hydrophilic PEG side chain, upon NP formulation, they should present on the NP surface for surface chemistry. We further functionalized these NPs with a cRGD tripeptide for targeting cancer cells in which integrin $\alpha_v\beta_3$ is overexpressed to enable cancer-targeted drug delivery.[14] The target CP-DOX NPs are denoted as TCP-DOX NPs. NPs self-assembled from PFVBT-*g*-PEG with the conjugation of the target moiety are denoted as TCP NPs. Figure 1B shows the UV/Vis absorption spectrum of a suspension of TCP-DOX NPs in water. The TCP-DOX NPs have an absorption maximum at 502 nm and an emission maximum at 598 nm (see Figure S2) with a Stokes shift of approximately 96 nm. The hydrodynamic diameter of TCP-DOX NPs was investigated by laser light scattering (LLS), which showed a volume average size of (120 ± 11) nm (Figure 1C). Transmission electron microscopy (TEM) was also conducted to study the morphology of the TCP-DOX NPs. The TCP-DOX NPs were clearly distinguished by their spherical shape (Figure 1C, inset) and had a mean diameter of 100 nm. The TCP-DOX NPs could be well-dispersed in water, phosphate-buffered saline (PBS), and DMEM cell medium (Dulbecco modified essential medium; Figure 1D), and their fluorescence and size remained unchanged even after incubation for 7 days at 37 °C, thus indicating good physical stability.

Next, we investigated the ROS production of the TCP-DOX NPs upon irradiation with light. ROS generation was determined by the fluorescence signal of a ROS-sensitive probe, dichlorofluorescein diacetate (DCF-DA). DCF-DA is nonfluorescent, but it can be rapidly oxidized to a fluorescent molecule (dichlorofluorescein, DCF) by ROS. Since PFVBT has a broad absorption spectrum, white light is able to induce the production of ROS. ROS production was more efficient with an increased power density (Figure 1E). Upon the irradiation of TCP-DOX NPs for 5 min, an 11.5-fold enhancement in the fluorescence intensity of DCF was detected at 530 nm, whereas the fluorescence intensity of the control groups without the NPs remained at the original level. When vitamin C (VC, a ROS scavenger) was added, the fluorescence from the DCF was significantly inhibited, thus further confirming ROS generation upon irradiation with light.

Since DOX was covalently conjugated to PFVBT by a thioketal linker, it was expected to show ROS-responsive drug release. To test this idea, we irradiated the TCP-DOX NPs with white light at a power density of 0.1 W cm^{-2} for

15 min before monitoring DOX release. As shown in Figure 1F, 25% of DOX was released in 1 h. In sharp contrast, NPs that were not subjected to irradiation with light showed negligible drug release (2.3%) during the same period of time. Irradiation of the TCP-DOX NPs with light at a power density of 0.25 W cm^{-2} for 15 min resulted in a slight increase in DOX release to 34% within 1 h. However, when VC was added, drug release was greatly inhibited to 6.9%, probably as a result of the decreased concentration of ROS around the NPs. Thus, TCP-DOX NPs are able to reduce premature drug release during circulation but can specifically enhance drug release upon irradiation with light.

Cancer-targeted drug delivery is a key requirement for future cancer therapy. To demonstrate the feasibility of the cancer-targeted delivery of DOX, we incubated TCP-DOX NPs with MDA-MB-231 and MCF-7 cancer cells expressing different levels of the $\alpha_v\beta_3$ integrin receptor and monitored the fluorescence of TCP-DOX NPs at different incubation time points. MDA-MB-231 cells with overexpressed integrin $\alpha_v\beta_3$ on the cellular membrane were chosen as integrin-positive cancer cells, and MCF-7 cells with low $\alpha_v\beta_3$-integrin expression were used as the negative control. After incubation for 4 h, both red fluorescence from TCP-DOX NPs in the cytoplasm and blue emission from Hoechst in the cell nucleus were observed in MDA-MB-231 cells; the red fluorescence was much brighter than in MCF-7 cells (see Figure S3). Semiquantitative fluorescence-intensity analysis of red fluorescence in these cells confirmed that the uptake of cRGD-modified NPs in MDA-MB-231 cells was 2.9-fold higher than that in MCF-7 cells (Figure 2A). We also noticed that the fluorescence intensity in both cells was gradually enhanced as the incubation time increased, and at each time point, a higher fluorescence was observed in MDA-MB-231 cells. The fluorescence signal was dramatically reduced in MDA-MB-231 cells when integrin was initially blocked by excess cRGD (Figure 2B). Semiquantitative fluorescence analysis in MDA-MB-231 cells demonstrated that there was a significant difference ($p < 0.05$) in the cellular uptake of TCP-DOX NPs before and after integrin blocking, thus indicating that the $\alpha_v\beta_3$ integrin receptor mediated cellular uptake.

We studied ROS production by TCP-DOX NPs inside the cancer cells under irradiation with light by using a cell-permeable fluorescent dye. Negligible fluorescence of DCF was observed when the cells were only loaded with DCF-DA or TCP-DOX NPs without light irradiation (see Figure S4). However, strong green fluorescence of DCF was observed after irradiation with light when the cells were loaded with TCP-DOX NPs. When VC (50 μM) was added, the fluorescence signal of DCF decreased significantly (see Figure S4D), which further confirmed the generation of ROS inside the cells during irradiation with light.

On the basis of the successful controlled drug release in solution and ROS generation in cells, on-demand drug release and combined chemotherapy/PDT were further carried out with MDA-MB-231 cells. As DOX is a commonly used anticancer drug which functions in the cell nucleus, we incubated free DOX, TCP NPs, and TCP-DOX NPs with MDA-MB-231 cells for 2 h in the dark and then irradiated the cells with light at a power density of 0.1 W cm^{-2} for 15 min.

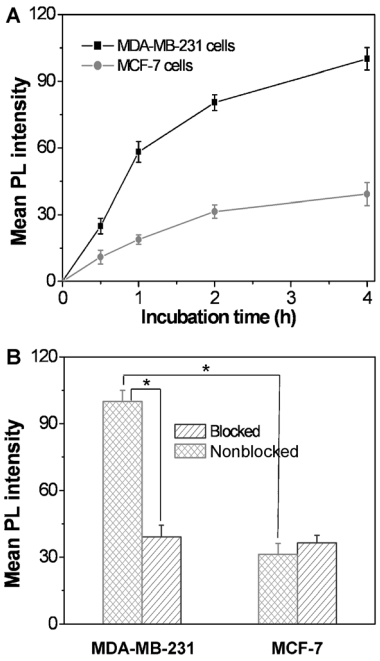

Figure 2. Evaluation of the targeting of TCP-DOX NPs to different cancer cells. A) Integrated photoluminescence (PL) intensity of TCP-DOX NPs in MDA-MB-231 and MCF-7 cells at different incubation times. B) PL intensity of TCP-DOX NPs in MDA-MB-231 and MCF-7 cells with and without pretreatment with cRGD (50 μM). The error is the standard deviation from the mean ($n = 3$, * is $P < 0.05$).

After further incubation for 3 h to ensure sufficient diffusion of the released DOX, the cells were examined by confocal microscopy. We found that both free DOX and sulfhydryl-modified DOX could quickly diffuse into the cell nucleus, which showed good coincidence with the Hoechst-stained nucleus (Figure 3A a,b; see also Figure S5). In contrast, no red fluorescence was detected in the cell nucleus for TCP NPs under both sets of conditions (Figure 3A c,d), thus indicating that TCP NPs are not able to enter the nucleus. However, in the case of TCP-DOX NPs before light irradiation, no red fluorescence was detected in the nucleus (Figure 3A e), whereas after exposure to light (0.1 W cm^{-2}, 15 min), red fluorescence from DOX was detected in the nucleus (Figure 3A f). In the presence of VC, this process was inhibited, and much weaker red fluorescence was observed in the nucleus, thus indicating that a lower amount of DOX was released (Figure 3A g,h). These results verify that the amount of DOX released is directly related to the generation of ROS from the NPs, thus demonstrating that ROS can cleave the drug conjugate in cells. We also carried out flow cytometry experiments to quantify the cellular uptake of DOX by MDA-MB-231 cell nuclei. We found that free DOX could quickly enter the cell nuclei (Figure 3B). For TCP-DOX NPs, after exposure to light, more DOX was found in the cell nuclei. However, in the presence of VC, this process was inhibited. These results further prove that the DOX can be released in the cytoplasm before migration into the nucleoplasm.

After irradiation with light, the early apoptosis of MDA-MB-231 cells was monitored with fluorescein isothiocyanate

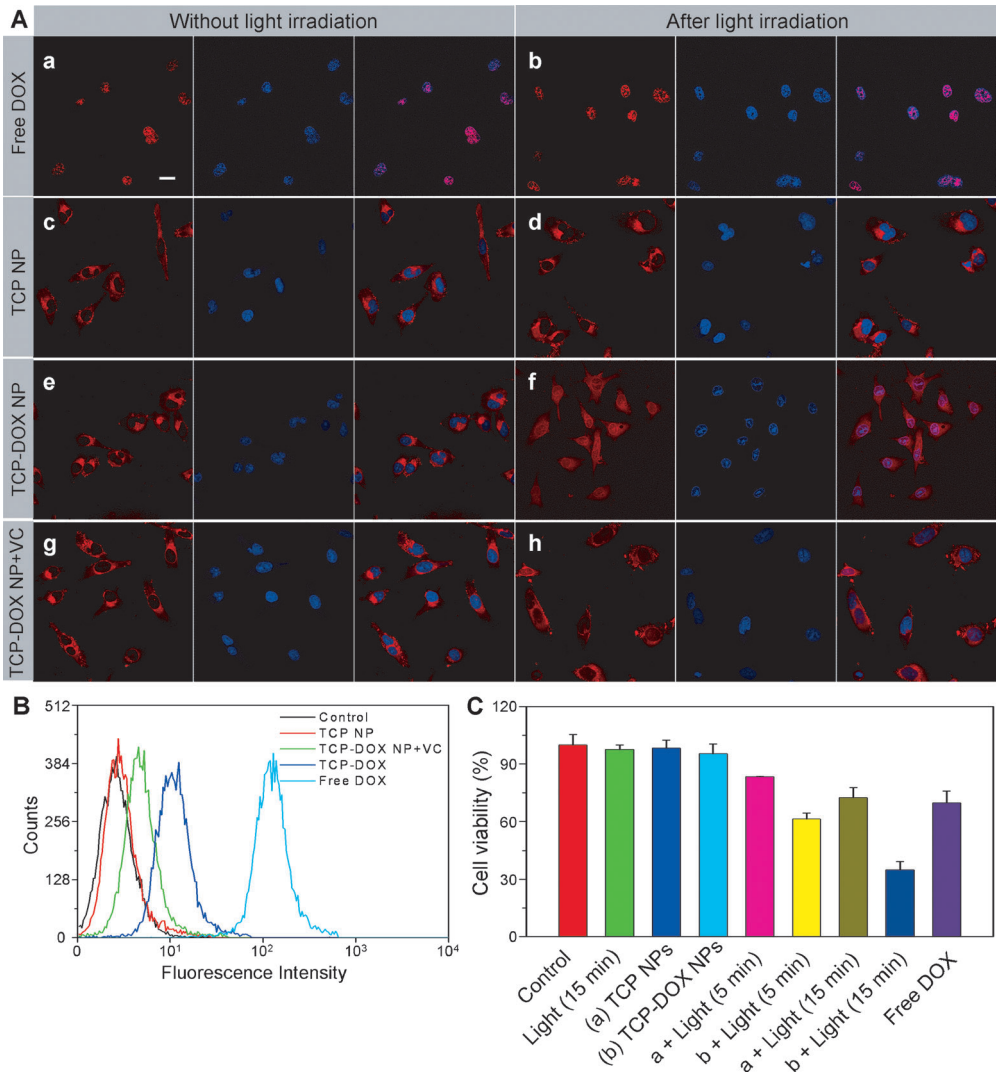

Figure 3. A) CLSM images of free DOX, TCP NPs, TCP-DOX NPs, and TCP-DOX NPs with the ROS scavenger VC incubated with MDA-MB-231 cells with and without irradiation with light. Red: fluorescence of TCP-DOX NPs; blue: cell nuclei stained by Hoechst 33342. All images share the same scale bar (20 μm). B) Flow cytometry analysis of the DOX fluorescence intensity in MDA-MB-231 cell nuclei. C) Viability of MDA-MB-231 cells incubated with free DOX, TCP NPs, and TCP-DOX NPs with (5 or 15 min) or without irradiation with light. Control samples were cells without any treatment.

(FITC)-tagged annexin V (see Figure S6). The in vitro cytotoxicity of TCP-DOX NPs under irradiation with light was then evaluated. MDA-MB-231 cells were incubated in the culture medium with free DOX, TCP NPs, and TCP-DOX NPs with and without exposure to light, and the cells were further incubated for 24 h in the dark. Treatment with light without NPs or with TCP NPs and TCP-DOX NPs without light did not result in a significant decrease in the cell viability, thus indicating the negligible toxicity of both types of NPs to MDA-MB-231 cells. In contrast, TCP NPs under irradiation with light showed some cytotoxicity to the cancer cells. This cytotoxicity could be explained by the production of ROS in the cells. However, incubation of the cells with TCP-DOX NPs under the same experimental conditions led to more evident cytotoxicity, which is thought to be due to the additional toxicity of released DOX. The increased toxicity with longer irradiation time can be attributed to the generation of more ROS and increased drug release. This finding agrees with the confocal laser scanning microscopy (CLSM) results that the drug release can be regulated by light. In contrast, TCP-DOX NPs show minimum toxicity to MCF-7 cells (see Figure S7) owing to their low cellular uptake. As a result, the combination of cRGD and light-triggered chemotherapy and PDT clearly makes it a very efficient light-controlled cancer-therapy system.

In summary, we designed a nanocarrier based on a PEGylated CPE that couples three modalities: targeted cancer-cell image with chemotherapy and PDT, both of which are controlled by irradiation by a single light source to enable on-demand cancer therapy. The carrier itself can generate ROS under irradiation with light and serve as a PDT agent. Meanwhile, the produced ROS can further activate drug release for on-demand chemotherapy. The light-controlled drug release was confirmed by CLSM and flow cytometry. In vitro cytotoxicity studies showed enhanced cell-viability inhibition for the combined therapy as compared to solely therapeutic activity. The results indicated that the theranostic nanoplatform is effective for on-demand PDT and chemotherapy. Currently, we are attempting to utilize the luminescence emitted from upconversion NPs under near-infrared laser irradiation as the ROS initiator. The use of near-infrared light rather than white light may further improve tissue penetration for in vivo applications.

Received: February 7, 2014
Published online: May 23, 2014

Keywords: conjugated polyelectrolytes · drug delivery · image-guided therapy · nanotechnology · photodynamic therapy

[1] a) D. E. Lee, H. Koo, I. C. Sun, J. H. Ryu, K. Kim, I. C. Kwon, *Chem. Soc. Rev.* **2012**, *41*, 2656; b) T. Lammers, S. Aime, W. E. Hennink, G. Storm, F. Kiessling, *Acc. Chem. Res.* **2011**, *44*, 1029.
[2] a) C. Wang, L. Cheng, Y. Liu, X. Wang, X. Ma, Z. Deng, Y. Li, Z. Liu, *Adv. Funct. Mater.* **2013**, *23*, 3077; b) Y. Zhang, J. Qian, D. Wang, Y. Wang, S. He, *Angew. Chem.* **2013**, *125*, 1186; *Angew. Chem. Int. Ed.* **2013**, *52*, 1148; c) E. S. Shibu, M. Hamada, N. Murase, V. Biju, *J. Photochem. Photobiol. C* **2013**, *15*, 53.
[3] R. Langer, *Nature* **1998**, *392*, 5.
[4] D. E. Dolmans, D. Fukumura, R. K. Jain, *Nat. Rev. Cancer* **2003**, *3*, 380.
[5] a) C. M. Peterson, J. M. Lu, Y. Sun, C. A. Peterson, J. G. Shiah, R. C. Straight, J. Kopecek, *Cancer Res.* **1996**, *56*, 3980; b) C. L. Peng, P. S. Lai, F. H. Lin, S. Y. H. Wu, M. J. Shieh, *Biomaterials* **2009**, *30*, 3614; c) A. Khdair, C. Di, Y. Patil, L. Ma, Q. P. Dou, M. P. V. Shekhar, J. Panyam, *J. Controlled Release* **2010**, *141*, 137; d) K. J. Son, H. J. Yoon, J. H. Kim, W. D. Jang, Y. Lee, W. G. Koh, *Angew. Chem.* **2011**, *123*, 12174; *Angew. Chem. Int. Ed.* **2011**, *50*, 11968.
[6] A. P. Castano, P. Mroz, M. X. Wu, M. R. Hamblin, *Proc. Natl. Acad. Sci. USA* **2008**, *105*, 5495.
[7] a) M. A. Cohen Stuart, W. T. S. Huck, J. Genzer, M. Müller, C. Ober, M. Stamm, G. B. Sukhorukov, I. Szleifer, V. V. Tsukruk, M. Urban, F. Winnik, S. Zauscher, I. Luzinov, S. Minko, *Nat. Mater.* **2010**, *9*, 101; b) E. Fleige, M. A. Quadir, R. Haag, *Adv. Drug Delivery Rev.* **2012**, *64*, 866.
[8] J. F. Gohy, Y. Zhao, *Chem. Soc. Rev.* **2013**, *42*, 7117.
[9] a) B. Liu, G. C. Bazan, *Chem. Mater.* **2004**, *16*, 4467 – 4476; b) A. Duarte, K. Y. Pu, B. Liu, G. C. Bazan, *Chem. Mater.* **2011**, *23*, 501; c) L. Feng, C. Zhu, H. Yuan, L. Liu, F. Lv, S. Wang, *Chem. Soc. Rev.* **2013**, *42*, 6620; d) K. Y. Pu, B. Liu, *Adv. Funct. Mater.* **2011**, *21*, 3408; e) H. Jiang, P. Taranekar, J. R. Reynolds, K. S. Schanze, *Angew. Chem.* **2009**, *121*, 4364; *Angew. Chem. Int. Ed.* **2009**, *48*, 4300.
[10] a) T. S. Corbitt, J. R. Sommer, S. Chemburu, K. Ogawa, L. K. Ista, G. P. Lopez, D. G. Whitten, K. S. Schanze, *ACS Appl. Mater. Interfaces* **2009**, *1*, 48; b) C. Zhu, Q. Yang, F. Lv, L. Liu, S. Wang, *Adv. Mater.* **2013**, *25*, 1203.
[11] a) D. S. Wilson, G. Dalmasso, L. Wang, S. V. Sitaraman, D. Merlin, N. Murthy, *Nat. Mater.* **2010**, *9*, 923; b) M. S. Shim, Y. Xia, *Angew. Chem.* **2013**, *125*, 7064; *Angew. Chem. Int. Ed.* **2013**, *52*, 6926.
[12] K. Y. Pu, K. Li, B. Liu, *Adv. Funct. Mater.* **2010**, *20*, 2770.
[13] a) S. Santra, C. Kaittanis, O. J. Santiesteban, J. M. Perez, *J. Am. Chem. Soc.* **2011**, *133*, 16680; b) P. Zou, Y. Yu, Y. A. Wang, Y. Zhong, A. Welton, C. Galban, S. Wang, D. Sun, *Mol. Pharm.* **2010**, *7*, 1974.
[14] U. Hersel, C. Dahmen, H. Kessler, *Biomaterials* **2003**, *24*, 4385.

